



TITANS

Research and Innovation Action (RIA)

Funded by the European Union. Views and opinions expressed are however those of the author(s) only and do not necessarily reflect those of the European Union or the European Atomic Energy Community ('EC-Euratom'). Neither the European Union nor the granting authority can be held responsible for them.

Start date : 2022-10-01 Duration : 36 Months



Samples for corrosion barriers.

Authors : Mrs. Raquel GONZALEZ (UPM), ETSI Industriales UPM, Elisabetta Carella, CIEMAT, Guillermo de la Cuerda Velazquez, ETSI Industriales UPM

TITANS - Contract Number: 101059408

Project officer: Angelgiorgio Iorizzo

Document title	Samples for corrosion barriers.
Author(s)	Mrs. Raquel GONZALEZ, ETSI Industriales UPM, Elisabetta Carella, CIEMAT, Guillermo de la Cuerda Velazquez, ETSI Industriales UPM
Number of pages	20
Document type	Deliverable
Work Package	WP02
Document number	D2.2
Issued by	UPM
Date of completion	2024-06-06 13:12:48
Dissemination level	Public

Summary

A large area sputtering setup for coatings fabrication has been adequate to allow the deposition of multilayer coatings in planar and non-planar geometries. Diverse coatings (Al_2O_3 , AlN and SiC) have been deposited by sputtering. The main aim was to optimize the sputtering process to achieve dense, amorphous, pinhole free and, well adhered to the substrate coatings. The optimization process consists on studying the morphology and microstructure of the coatings as a function of the sputtering parameters (Ar flow rate, partial oxygen or nitrogen flow rate, sample bias, plasma power...). We also investigated the influence of a bonding layer on the adhesion of the coatings to the Eurofer substrate. We have ruled out continuing with the fabrication of AlOx because it has been observed, that in these coatings Li penetrates throughout the entire thickness in a significant amount which may be related to the large reactivity of AlOx with Li which may lead to solid state reaction whose result is the formation of lithium aluminate phases. Under neutron irradiation this lithium will transmute into He and T which could have some important drawbacks in the application of Al_2O_3 as TPBs both from the safety and from the technological point of view. We have carried out part of the optimization process for the deposition of AlNx coating and their adhesion to the substrate. One of the most dense, homogeneous and amorphous deposited AlNx coating has been submitted to a COES test. Preliminary results indicate that the coatings completely delaminated from the Eurofer substrate, which may be related, among other factors on the insufficient adhesion of the coating to the substrate. Further efforts are oriented to improve this parameter are foreseen. We have performed part of the optimization process for the deposition of SiC coating and their adhesion to the substrate. We have identified the sputtering conditions, which leads to coatings with the desired properties and well adhered to the Eurofer. We have investigated the behaviour of those coatings under thermal cycling concluding (from XRD data) that they remain amorphous after the thermal cycling and well adhered to the Eurofer. We have deposited some SiC coatings to further investigate their behaviour as permeation and corrosion (immersion in PbLi) barriers.

Approval

Date	By
2024-06-06 13:14:38	Dr. Moreno CARLOS (CIEMAT)
2024-06-13 17:29:09	Mrs. Elodie BERNARD (CEA)

Disclaimer

Funded by the European Union. Views and opinions expressed are however those of the author(s) only and do not necessarily reflect those of the European Union or the European Atomic Energy Community ('EC-Euratom'). Neither the European Union nor the granting authority can be held responsible for them.



Table of Contents

1	Adequacy of the sputtering setup.....	8
2	Fabrication of Al₂O₃ coatings	8
2.1	Optimization of the fabrication process	8
2.2	Optimization of the fabrication process	10
3	Fabrication of AlN_x coatings.....	12
3.1	Optimization of the fabrication process	12
3.1.1	Influence of the sputtering parameters on the morphology of the coatings.....	12
3.1.2	Influence of etching on adhesion of the coating to the substrate	14
3.2	Characterization of AlN _x coatings after exposure to PbLi: preliminary results	15
4	Fabrication of SiC coatings.....	16
4.1	Optimization of the fabrication process	16
4.1.1	Influence of the sputtering parameters on the morphology of the coatings.....	16
4.2	Thermal cycling experiments.....	18

List of Figures

Figure 1. Photography of the sputtering setup after being commissioned to allow the deposition of multilayer coatings in planar and non-planar geometries: a) exterior view, b) interior view.	8
Figure 2. Cross sectional SEM Images for diverse AlO _x coatings deposited by reactive sputtering at different O flow rates: 5.30 sccm a), 10.0 sccm (b) and 19.9 sccm (c)	9
Figure 3. Cross sectional SEM images for diverse AlO _x coatings deposited by reactive sputtering at different pulse frequencies: 250 kHz a), 200 kHz b), 100 kHz c); all of them have been deposited at φ _{O₂} =5 sccm.....	10
Figure 4. Measured and simulated ion-beam analysis spectra for Al ₂ O ₃ coatings deposited on EUROFER steels exposure to PbLi under the conditions shown in Table 1.....	11
Figure 5. SEM cross-sectional images for the series 3 (a – c, 200 kHz) and series 4 (e – g, 100 kHz) AlN coatings	13
Figure 6. Optical micrographs of the indents caused in the DBRCi tests on samples. The adhesion strength HF values are shown in each case.....	14
Figure 7. Photography (a) and optical microscopy images (b) of the AlN _x coating surface after the corrosion test.....	15

Figure 8. 3D topographic map of the AlN_x sample submitted to PbLi static corrosion.	15
Figure 9. Top view and cross-sectional SEM pictures of SiC coatings deposited on naked (100) Si substrate at diverse Ar flow rate.....	17
Figure 10. XRD patterns for SiC coatings sputtered at different Φ_{Ar} of 40 (a), 19 (b) and 9 (c) sccm before (blue line) and after thermal cycling (red line).	19

List of Tables

Table 1. Overview of the sample codes, deposition parameters, coating thickness and deposition rate	9
Table 2. Sample code and thickness for diverse Al_2O_3 coatings exposure to PbLi under stagnant conditions, at a temperature of 550 °C, for times of 4000 and 7000 h.....	10
Table 3. Sample code, sputtering parameters, thickness, and deposition rate for the deposited AlN_x coatings.....	13
Table 4. Sample code, Ar flow rate and, bias voltage applied to the Eurofer substrate during coating deposition and bonding layer	16

Abbreviation and Acronyms

Acronym	Description
DBR	Daimler Benz Rockwell
IBA	Ion beam analysis
LM	Liquid metals
NRA	Nuclear reaction analysis
OM	Optical microscopy
PLD	Pulsed laser deposition
RBS	Rutherford backscattering spectroscopy
SEM	Scanning electron microscopy
SIMS	Secondary ion mass spectroscopy
TPB	Tritium permeation barriers
WP	Work package

Executive Summary

A large area sputtering setup for coatings fabrication has been adequate to allow the deposition of multilayer coatings in planar and non-planar geometries.

Diverse coatings (Al_2O_3 , AlN and SiC) have been deposited by sputtering. The main aim was to optimize the sputtering process to achieve dense, amorphous, pinhole free and, well adhered to the substrate coatings. The optimization process consists on studying the morphology and microstructure of the coatings as a function of the sputtering parameters (Ar flow rate, partial oxygen or nitrogen flow rate, sample bias, plasma power...). We also investigated the Influence of a bonding layer on the adhesion of the coatings to the Eurofer substrate.

We have ruled out continuing with the fabrication of AlO_x because it has been observed, that in these coatings Li penetrates throughout the entire thickness in a significant amount which may be related to the large reactivity of AlO_x with Li which may lead to solid state reaction whose result is the formation of lithium aluminate phases. Under neutron irradiation this lithium will transmute into He and T which could have some important drawbacks in the application of Al_2O_3 as TPBs both from the safety and from the technological point of view.

We have carried out part of the optimization process for the deposition of AlN_x coating and their adhesion to the substrate. One of the most dense, homogeneous and amorphous deposited AlN_x coating has been submitted to a COES test. Preliminary results indicate that the coatings completely delaminated from the Eurofer substrate, which may be related, among other factors on the insufficient adhesion of the coating to the substrate. Further efforts are oriented to improve this parameter are foreseen.

We have performed part of the optimization process for the deposition of SiC coating and their adhesion to the substrate. We have identified the sputtering conditions, which leads to coatings with the desired properties and well adhered to the Eurofer. We have investigated the behaviour of those coatings under thermal cycling concluding (from XRD data) that they remain amorphous after the thermal cycling and well adhered to the Eurofer. We have deposited some SiC coatings to further investigate their behaviour as permeation and corrosion (immersion in PbLi) barriers.

Keywords

Coatings, sputtering, tritium barriers, corrosion barriers, PbLi.



Introduction

Next generation of some key energy sources (generation IV fission, fusion and concentrated solar power) are requested to provide an increased overall efficiency at acceptable costs that will require increasing operation temperature. For that purpose, liquid metals (LM) are proposed as high temperature heat transfer fluids, since they offer much better properties than traditional coolants. Their main advantages are chemical stability at high operation temperature largely improved heat transfer when compared to conventional fluids, as well as their ability to work under harsh environments. However, LM are highly corrosive, therefore a major issue is the corrosion protection of structural materials in contact with them. Moreover, in nuclear fission (generation IV) [1] and fusion reactors [2], it is also necessary to prevent tritium leakage allowing a proper and safe reactor operation.

One cheap and easy way to overcome the tritium leakage and corrosion problem is to cover the steel substrate with a coating [3][4]. Such a solution would prevent tritium leakage and improve the corrosion behaviour of the system (coating/steel) while keeping the structural properties and low cost of the steel. Therefore, in nuclear reactors coatings must have two different functions: act as tritium permeation barriers and protect the steel against corrosion.

In this project we propose to fabricate diverse type of dense, amorphous, pinhole free and, well adhered to the Eurofer substrate coatings by sputtering to prevent, simultaneously, tritium permeation and corrosion.

We chose sputtering as fabrication method because it is an easy control, environmentally friendly, versatility, scalable and low-cost technique which allows tuning the coating properties by properly selecting the sputtering parameters and also lets improving the adhesion of the coating to the surface which is one of the most critical points.

1 Adequacy of the sputtering setup

During the first months the sputtering setup for coatings fabrication has been adequate to allow the deposition of multilayer coatings. To do that a new rotating sample holder has been designed and commissioned and two new magnetrons have been introduced into the deposition chamber. Moreover, a new gas inlet has been installed to allow fabricate, using reactive sputtering, diverse nitrides and carbides. Figure 1 shows a photography of the sputtering setup into its actual configuration. This configuration allows the system to cover planar and non-planar geometries. Thus, it allows covering planar but also non-planar surfaces.

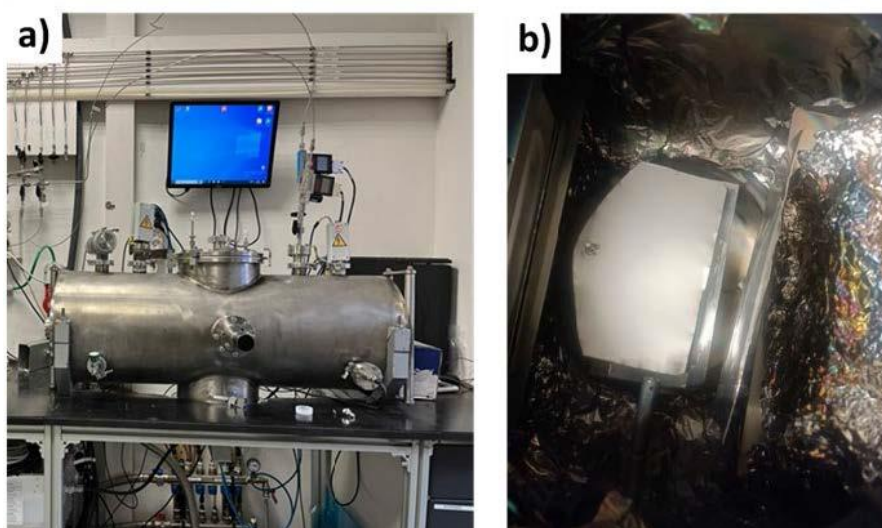


Figure 1. Photography of the sputtering setup after being commissioned to allow the deposition of multilayer coatings in planar and non-planar geometries: a) exterior view, b) interior view.

2 Fabrication of Al_2O_3 coatings

2.1 Optimization of the fabrication process

We have investigated the capabilities of sputtering to fabricate dense, amorphous, pinhole free and, well adhered to the Eurofer substrate AlO_x coatings. To do that firstly we have investigated the influence of the sputtering parameters on the morphology and elemental composition of the coatings in order to optimize the sputtering process. For this purpose, four series of AlO_x were deposited from an aluminium commercial target in the presence of an $\text{Ar}+\text{O}_2$ atmosphere at room temperature with varying pulsed DC power source parameters. In each series the total flow rate, pressure, the target-substrate distance and the deposition power were kept constant at $8 \cdot 10^{-3}$ mbar, 13 cm and 400 W respectively, whereas the oxygen partial flow rate (ϕ_{O_2}) was varied from around 5 to 20 sccm. Between series,

the power source parameters (time off, frequency) are modified.

All coatings were deposited on single crystalline (100) Si substrates, cleaned using a sequence of washing with alkaline detergents, rinsing with water, cleaning with isopropanol and air-drying. The deposition time was 60 min.

An overview of the sample codes, deposition parameters, coating thickness and deposition rate is listed in Table 1.

Sample	T _{off} (μs)	Frequency (kHz)	Duty Cycle (%)	Voltage (V)	ΦO ₂ (sccm)	Thickness (μm)	Deposition rate (nm/min)
S3AlO1	2.9	150	56.5	252	3	5.46 ± 0.04	91.04 ± 0.7
S3AlO2	2.9	150	56.5	169	9	0.45 ± 0.02	7.48 ± 0.31
S3AlO3	2.9	150	56.5	160	22	0.23 ± 0.03	3.89 ± 0.60
S3AlO1	1.6	250	60	188	5	0.50 ± 0.03	8.39 ± 0.50
S3AlO2	1.6	250	60	190	10	0.39 ± 0.02	6.47 ± 0.27
S3AlO3	1.6	250	60	180	25	0.34 ± 0.03	5.73 ± 0.48
S3AlO1	1.6	200	68	210	5	0.63 ± 0.05	10.47 ± 0.79
S3AlO2	1.6	200	68	200	10	0.43 ± 0.03	7.09 ± 0.45
S3AlO3	1.6	200	68	195	20	0.39 ± 0.07	6.57 ± 1.12
S3AlO1	0.4	100	95	280	5	0.37 ± 0.06	6.23 ± 1.08

Table 1. Overview of the sample codes, deposition parameters, coating thickness and deposition rate

Figure 2 shows cross-sectional SEM images for samples deposited at different ϕ_{O_2} using the same power source parameters.

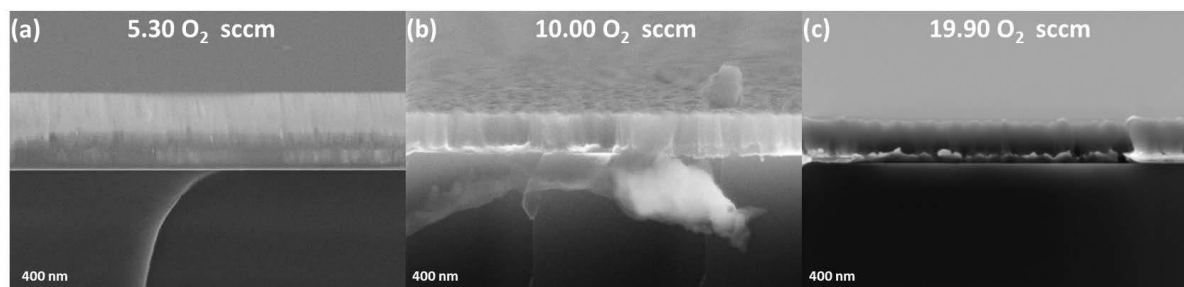


Figure 2. Cross sectional SEM Images for diverse AlO_x coatings deposited by reactive sputtering at different O flow rates: 5.30 sccm a), 10.0 sccm (b) and 19.9 sccm (c)

Compact and dense coatings are achieved at low φ_{O_2} . Increasing the φ_{O_2} leads to a clear transition from dense and homogeneous morphology to a columnar-like.

Figure 3 shows cross-sectional SEM images for samples deposited at different pulse frequencies using the same φ_{O_2} (5 sccm). It is observed that working at low frequencies also favours the deposition of compact and homogeneous coatings.

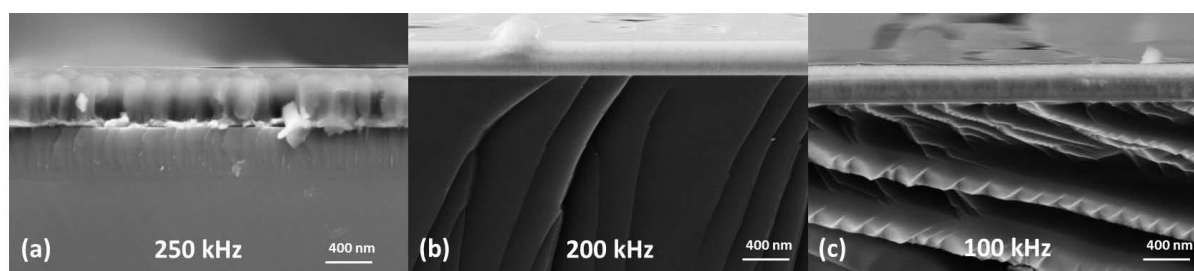


Figure 3. Cross sectional SEM images for diverse AlO_x coatings deposited by reactive sputtering at different pulse frequencies: 250 kHz a), 200 kHz b), 100 kHz c); all of them have been deposited at $\varphi_{O_2}=5$ sccm.

Elemental composition analysis, IBA, data show that all coatings are overstoichiometric (oxygen content of 60 at. %). No significant dependence of the elemental composition on φ_{O_2} is observed in the studied range, suggesting the coatings are saturated with oxygen.

2.2 Optimization of the fabrication process

Simultaneously to the optimization of the fabrication process for AlO_x coatings by sputtering, we have characterized amorphous and dense Al_2O_3 coatings deposited by pulsed laser deposition (PLD) on EUROFER after exposure to PbLi under stagnant conditions, at a constant temperature of 550 °C, for different times (4000 h, 7000 h), at ENEA – RACHEL facility [5].

Sample	Thickness (μm)	Time (h)	PbLi exposure temperature ($^{\circ}\text{C}$)	Conditions
S1	3	7000	550	Stagnant
S2	5	7000	550	Stagnant
S3	3	4000	550	Stagnant

Table 2. Sample code and thickness for diverse Al_2O_3 coatings exposure to PbLi under stagnant conditions, at a temperature of 550 °C, for times of 4000 and 7000 h.

The PbLi exposure conditions together with the sample code and thickness are listed in Table 1. More details about the coating deposition procedure and coatings properties are described in references [6][7].

The elemental composition of the coatings was characterized with secondary ion mass spectroscopy (SIMS) and ion beam analysis (IBA) techniques. Figure 4 shows measured and simulated ion-beam analysis spectra for the diverse coatings.

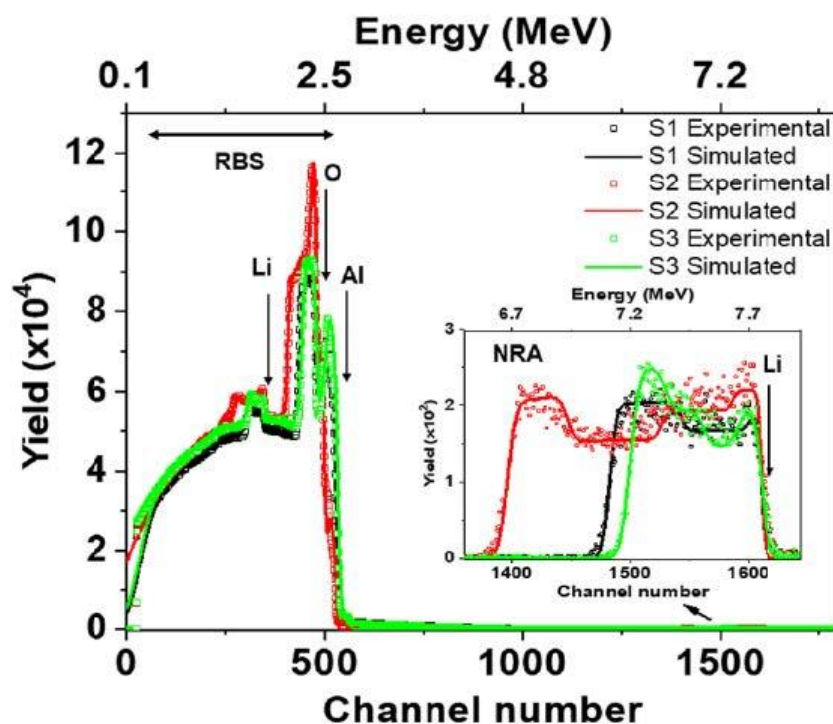


Figure 4. Measured and simulated ion-beam analysis spectra for Al_2O_3 coatings deposited on EUROFER steels exposure to PbLi under the conditions shown in Table 1.

In agreement with SIMS data (not shown), IBA spectra evidence the presence of Li in all the studied coatings, distributing from the coating surface to the EUROFER substrate along the whole coating thickness. The Li content is larger at the coating surface and at the coating/EUROFER interface than at any other point within the coating. Li contents of up to 14 at. % were calculated in the coating region close to coating/EUROFER interface [8].

Under neutron irradiation, Li will transmute into He and T which could have some important drawbacks in the application of Al_2O_3 as TPBs both from the safety and from the technological point of view.

Because of these results we decide to stop the fabrication of AlO_x coatings, looking for alternative materials.

3 Fabrication of AlN_x coatings

3.1 Optimization of the fabrication process

3.1.1 Influence of the sputtering parameters on the morphology of the coatings

Diverse AlN_x coatings have been deposited by reactive magnetron sputtering from an aluminium commercial target in the presence of an Ar+N₂ atmosphere. Coatings were deposited on single crystalline (100) Si substrates at room temperature and at a constant pulsed-DC power was of 400W. The total flow rate, pressure and the target–substrate distance were kept constant at 80 sccm, $8 \cdot 10^{-3}$ mbar, and 13 cm respectively, whereas the nitrogen flow (ϕ_{N_2}) was varied from ~5 to ~20 sccm. The power source parameters (frequency, time off, toff) were also varied between series. The deposition time was 60 minutes for all samples.

Coatings were deposited on three different substrates: single crystalline (100) Si and polished steels (HSS and EUROFER). Samples deposited on (100) Si were used for the characterization purposes (elemental composition and morphology), whereas those samples deposited on steel were the ones selected to study the adhesion of the coatings to the substrate and their resistance to corrosion.

Sample	T _{off} (μs)	Frequency (kHz)	Duty Cycle (%)	Voltage (V)	ΦN ₂ (sccm)	Thickness (μm)	Deposition rate (nm/min)
S3AIN1	1.6	200	68	223	5	2.48±0.1	41.27±1.67
S3AIN2	1.6	200	68	197	10	1.67±0.12	27.87±1.85
S3AIN3	1.6	200	68	188	20	0.77±0.02	12.90±0.37
S4AIN1	1	100	90	275	5	2.78±0.06	46.39±0.94
S4AIN2	1	100	90	249	10	1.90±0.04	31.60±0.65
S4AIN3	1	100	90	232	20	0.88±0.01	14.69±10.23
S6AIN1	1.6	200	68	199 (25V bias)	10	2.06±0.04	34.36±0.67
S6AIN2	1.6	200	68	203	10	2.07±0.05	29.53±0.79

				(50V bias)			
S6AIN3	1.6	200	68	202 (75V bias)	10	1.82±0.03	30.26±0.46

Table 3. Sample code, sputtering parameters, thickness, and deposition rate for the deposited AlN_x coatings.

Prior to deposition the substrates were cleaned with alkaline detergent rising with water, immersion in isopropanol and air drying.

As in the previous section, firstly the influence of the sputtering parameters on the morphological and microstructural properties of the coatings was investigated. An overview of the sample code together with sputtering parameters, sample thickness and deposition rate, is shown in Table 3.

Figure 4 shows cross sectional SEM images for samples deposited at different ϕ_{N_2} at two frequencies (200kHz and 100 kHz).

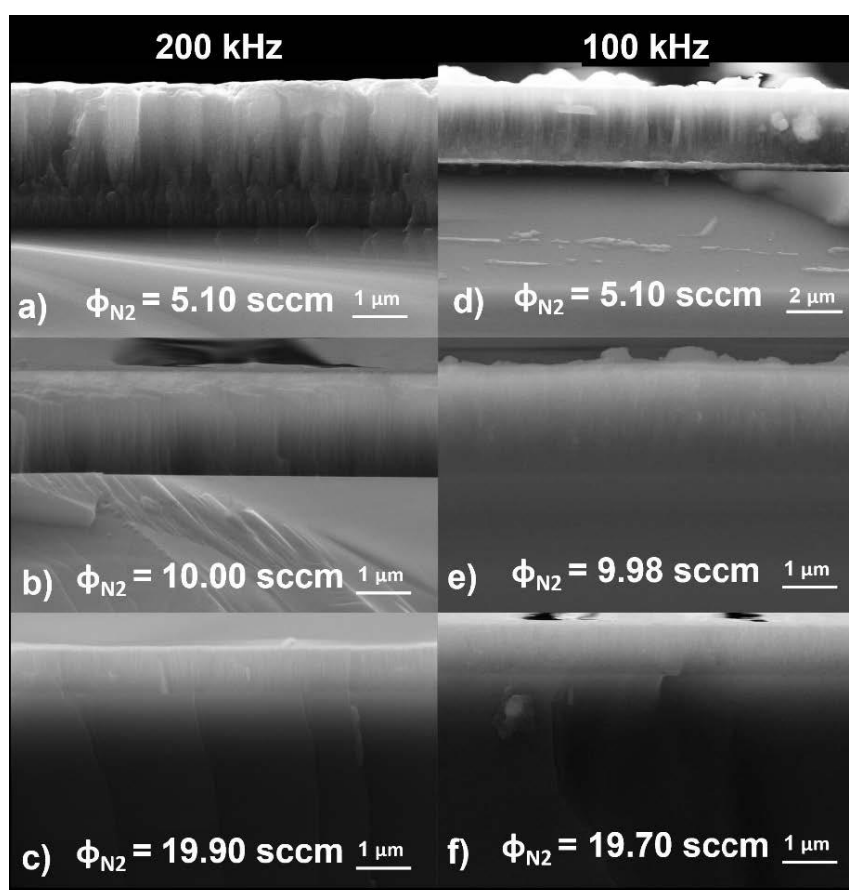


Figure 5. SEM cross-sectional images for the series 3 (a – c, 200 kHz) and series 4 (e – g, 100 kHz) AlN coatings

A clear transition from columnar to a dense and homogeneous morphology is observed when increasing φ_{N_2} . No significant influence of the frequency on the coating morphology is observed.

Elemental composition data show that the nitrogen content in the coating increases from ~ 33 at. % up to ~ 52 at. % when rising the φ_{N_2} in the chamber from 5 to 10 sccm. Increasing φ_{N_2} above 10 sccm, does not change the stoichiometry but changes the morphology, promoting coating densification.

3.1.2 Influence of etching on adhesion of the coating to the substrate

We have studied the influence of performing argon glow discharge plasma pre-treatment of the substrate on the coating adhesion to the substrate. For this purpose, two samples were deposited under the same conditions (select to obtain dense, homogeneous and amorphous coatings) on two stainless steel (SS) 316L mirror-polished substrates. Prior to any pre-treatment, the substrates were cleaned using a sequence of washing with alkaline detergents, rinsing with water, cleaning with isopropanol and air-drying. After that, prior to the coating deposition, one of the substrates underwent an etching treatment for 30min in which an Ar+ glow discharge was established at the substrate using a DC-pulsed bias voltage of -75 V, a frequency of 150 kHz and a pulse length of $2.9 \mu\text{s}$ and an Ar flow of 40 sccm.

The adhesion is then characterized by DBRCi test. Results are shown in Figure 6.

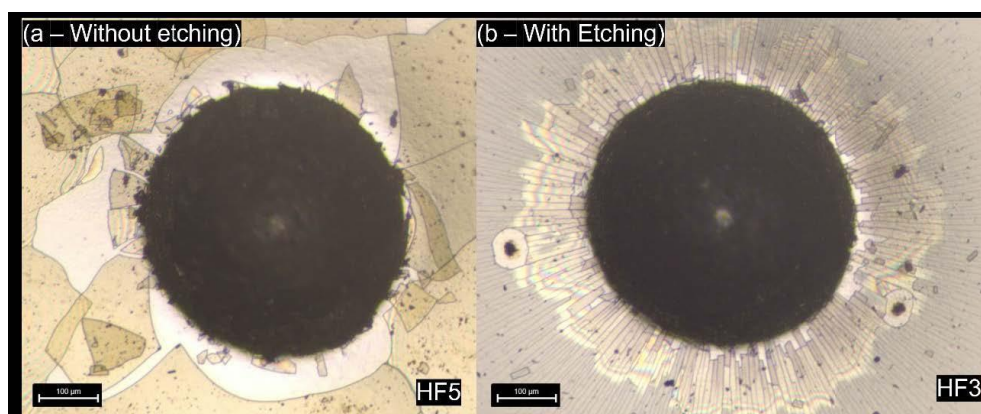


Figure 6. Optical micrographs of the indents caused in the DBRCi tests on samples. The adhesion strength HF values are shown in each case.

Ar etching greatly improves the adhesion of the coating to the substrate (from HF5 to HF3). However, there is still room for improving the deposition process.

3.2 Characterization of AlN_x coatings after exposure to PbLi: preliminary results

Keeping in mind that there is still room for improvement, in the sputtering process, one of the AlN_x coating (dense, homogeneous and amorphous) were submitted to corrosion by PbLi under stagnant conditions for 336h (2 weeks) at CIEMAT. Images of the sample surface after corrosion are shown in Figure 7.

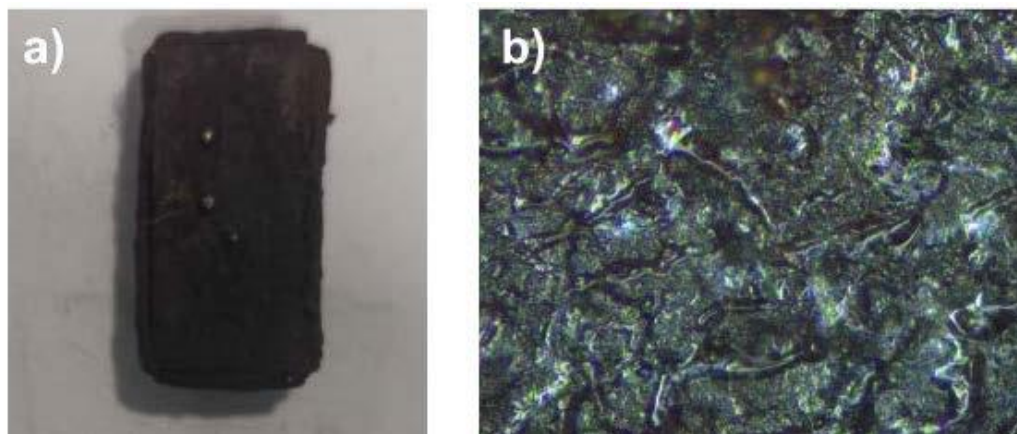


Figure 7. Photography (a) and optical microscopy images (b) of the AlN_x coating surface after the corrosion test.

The optical images reveal a significant increase in roughness, and apparently there is no coating left. This is further corroborated 3D topographic map of the sample (see Figure 8), where variations in height of $\sim 220 \mu\text{m}$ indicating that the $2 \mu\text{m}$ -thick coating did not survive the PbLi corrosion test.

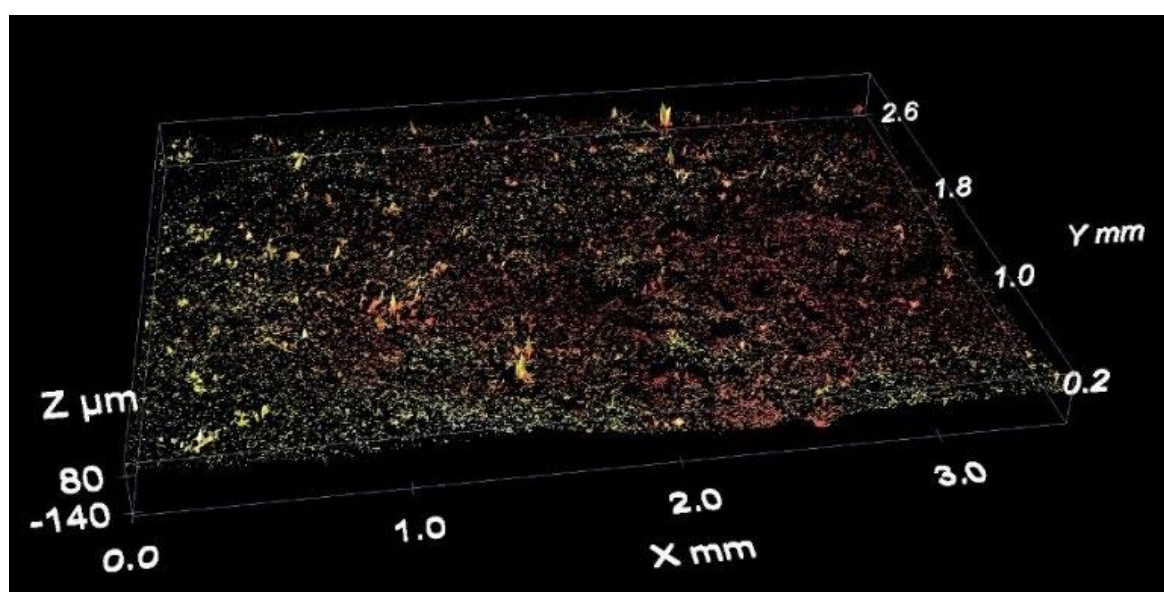


Figure 8. 3D topographic map of the AlN_x sample submitted to PbLi static corrosion.

4 Fabrication of SiC coatings

4.1 Optimization of the fabrication process

4.1.1 Influence of the sputtering parameters on the morphology of the coatings

Si coatings were deposited on (100) Si and on polished Eurofer substrate.

Three series of SiC coatings have been deposited by sputtering under diverse deposition conditions. In all of them, SiC coatings were deposited by RF magnetron sputtering from a pure (99.95%) SiC commercial target at a plasma power of 300 W and, at room temperature. A summary of the sample codes and deposition conditions is illustrated in Table 4.

Sample	Φ_{Ar} (sccm)	Bias voltage (V)	Bonding
S1SiC1	112	0	No
S1SiC2	59.3	0	No
S1SiC3	39.6	0	No
S1SiC4	18.9	0	No
S1SiC5	9.6	0	No
S2SiC1	18.9	0	No
S2SiC2	18.9	0	Yes
S3SiC1	39.6	30	Yes
S3SiC2	39.6	60	Yes
S3SiC3	39.6	90	Yes

Table 4. Sample code, Ar flow rate and, bias voltage applied to the Eurofer substrate during coating deposition and bonding layer

In the first series, SiC coatings were deposited directly on naked substrates. In this series, the Ar flow rate (Φ_{Ar}) was varied from 18.9 sccm to 112 sccm to study their influence on the sample morphology and microstructure. Figure

9 shows top view and cross-sectional SEM pictures of the deposited SiC coatings.

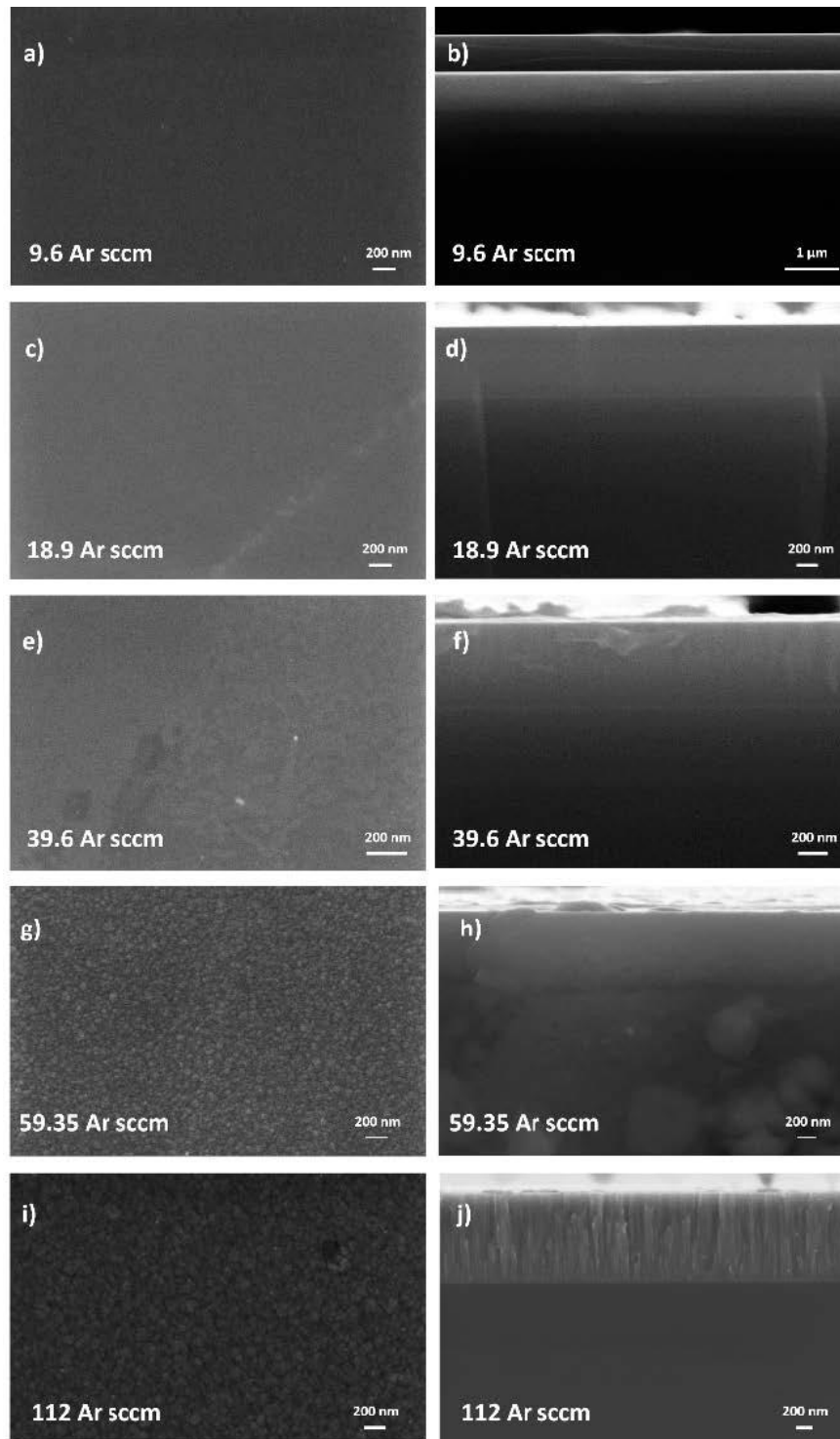


Figure 9. Top view and cross-sectional SEM pictures of SiC coatings deposited on naked (100) Si substrate at diverse Ar flow rate.

A transition from homogeneous to columnar morphology is observed with increasing Φ_{Ar} . Homogeneous coatings are obtained at $\Phi_{Ar} \leq 60$ sccm (5.5×10^{-3} mbar).

In the second series, the aim was to investigate the influence of having a bonding layer in the adhesion of the coating to the substrate. To do that Φ_{Ar} was fixed at 18.9 sccm and a Ti bonding layer with a thickness of ~20 nm was deposited on the bare HSS substrate. Immediately after that the SiC coating was deposited in the same chamber. A clear improvement in adhesion from HF5 to HF1 is observed when a Ti bonding layer is used.

In the third series, the influence of the sample bias on the morphology and microstructure of the coating was investigated. To do that Φ_{Ar} was fixed at 39.6 sccm and the bias of 30, 60 and 110 V was applied to the substrate during the SiC coating deposition. In this series a Ti bonding layer with a thickness of ~20 nm was deposited before the deposition of the SiC coating. These samples are under investigation.

4.2 Thermal cycling experiments

The stability of the samples under thermal cycling was investigated. To do that, SiC coatings deposited by RF magnetron sputtering at a plasma power of 300 W, at room temperature and, at several Φ_{Ar} (40, 19 and 9 sccm) were subjected to 50 thermal cycles up to a temperature of 450 °C. This temperature was selected because of two reasons. On the one hand it is similar to that expected in the BB location, on the other it is low enough to avoid any change in the Eurofer steel. Each of thermal cycles consists of a heating up and a cooling down phase in which the temperature was increased from 150 °C to 450 °C and vice versa. In the warm up phase, the rate was 22 °C/min and, in the cooling down 67°C/min. The thermal cycles were carried out in Ar at a pressure of 0,8 bar. The morphological and microstructural properties of the samples as well as, the adhesion of the samples to the Eurofer substrates were investigated prior to and after thermal cycling by means of, SEM, XRD and nanoscratch, respectively. Figure 10 shows XRD patterns for SiC coatings sputtered at different Φ_{Ar} . For comparison diffraction peaks corresponding to α -Fe and Hex SiC phases have been included in this figure.

These data evidence that either the spectra for the as-deposited or those for the thermally cycled coating do not present any diffraction maximum, which indicates their amorphous character.

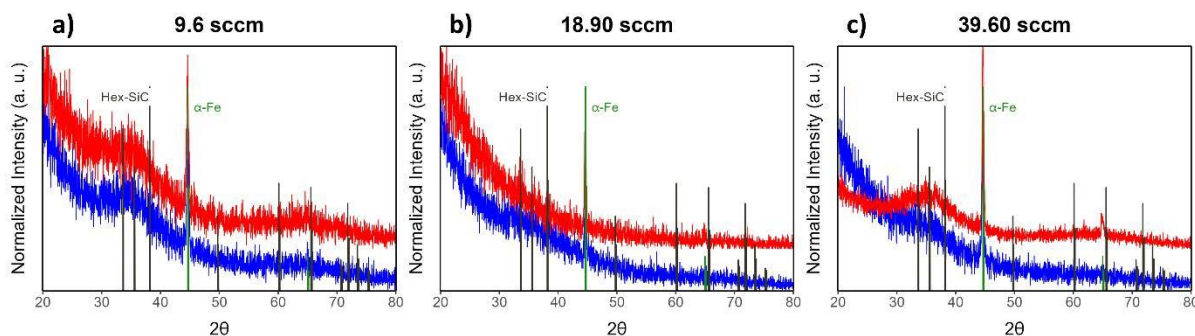


Figure 10. XRD patterns for SiC coatings sputtered at different ϕ_{Ar} of 40 (a), 19 (b) and 9 (c) sccm before (blue line) and after thermal cycling (red line).

Preliminary nanoscratch results indicate no deterioration of the adhesion of the coating to the substrate after thermal cycling.

Conclusion

A large area magnetron sputtering setup has been adequate to allow the deposition of multilayer coatings in planar and non-planar geometries as well as, several nitrides and carbides when used in the reactive mode configuration.

We have ruled out continuing with the fabrication of AlO_x because it has been observed, that in these coatings Li penetrates throughout the entire thickness in a significant amount (up to 14 at. % according to IBA data). Under neutron irradiation this lithium will transmute into He and T which could have some important drawbacks in the application of these coatings as TPBs both from the safety and from the technological point of view.

We have carried out part of the optimization process for the deposition of AlN_x coating and their adhesion to the substrate. Further work is needed to achieve dense, amorphous, pinhole free and, well adhered to the substrate coatings. In particular, we are going to focus on improving the adhesion of the AlN_x coating to the Eurofer so far, based on DBRCi data, we have only achieved HF3 adhesion.

We have carried out partially the optimization process for the deposition of SiC coating and their adhesion to the substrate. We have identified the sputtering conditions, which leads to coatings with the desired properties. These coatings have been demonstrated to remain amorphous and well adhered to the Eurofer substrate after thermal cycles. Further research on their behaviour as permeation and corrosion (immersion in PbLi) barriers is going to be performed.

Bibliography

- [1] C.W. Forsberg, S. Lam, D.M. Carpenter, D.G. Whyte, R. Scarlat, C. Contescu, L. Wei, J. Stempien, E. Blandford, Tritium Control and Capture in Salt-Cooled Fission and Fusion Reactors: Status, Challenges, and Path Forward, *Nucl. Technol.* 197 (2017) 119–139. <https://doi.org/10.13182/NT16-101>.
- [2] R.A. Causey, R. Karnesky, C. San Marchi, Tritium Barriers and Tritium Diffusion in Fusion Reactors, *Compr. Nucl. Mater.* 4 (2012) 511–549. <https://doi.org/10.1016/B978-0-08-056033-5.00116-6>.
- [3] T. Hernández, F.J. Sánchez, A. Moroño, E. León-Gutiérrez, M. Panizo-Laiz, M.A. Monclus, R. González-Arrabal, Corrosion behavior of diverse sputtered coatings for the helium cooled pebbles bed (HCPB) breeder concept, *Nucl. Mater. Energy.* 25 (2020) 100795. <https://doi.org/10.1016/j.nme.2020.100795>.
- [4] T. Hernández, F.J. Sánchez, F. Di Fonzo, M. Vanazzi, M. Panizo, R. González-Arrabal, Corrosion protective action of different coatings for the helium cooled pebble bed breeder concept, *J. Nucl. Mater.* 516 (2019) 160–168. <https://doi.org/10.1016/j.jnucmat.2019.01.009>.
- [5] S. Bassini, Coolant Chemistry Control in Heavy Liquid Metal Cooled Nuclear Systems, Doctoral Thesis, Alma Mater Studiorum - Università di Bologna, 2017. <https://doi.org/10.6092/unibo/amsdottorato/8026>.
- [6] M. Utili, S. Bassini, S. Cataldo, F. Di Fonzo, M. Kordac, T. Hernandez, K. Kunzova, J. Lorenz, D. Martelli, B. Padino, A. Moroño, M. Tarantino, C. Schroer, G.A. Spagnuolo, L. Vala, M. Vanazzi, A. Venturini, Development of anti-permeation and corrosion barrier coatings for the WCLL breeding blanket of the European DEMO, *Fusion Eng. Des.* 170 (2021) 112453. <https://doi.org/10.1016/j.fusengdes.2021.112453>.
- [7] F. Ferré, M. Ormellese, F. Fonzo, M. Beghi, Advanced Al₂O₃ coatings for high temperature operation of steels in heavy liquid metals: A preliminary study, *Corros. Sci.* 77 (2013) 375–378. <https://doi.org/10.1016/j.corsci.2013.07.039>.
- [8] R. González-Arrabal, E. Carella, F.J. Sánchez, G. de la Cuerda-Velázquez, G. García, J.M. Perlado, T. Hernández, Characterization of the lithium concentration and distribution as a function of depth for alumina coatings after exposure to PbLi, *J. Nucl. Mater.* 586 (2023) 154688. <https://doi.org/10.1016/j.jnucmat.2023.154688>.